



## Trajectory-based identification of critical instantaneous decision events at mixed-flow signalized intersections

Yanning Wei, Keping Li, Keshuang Tang\*

College of Transportation Engineering, Tongji University, Shanghai, 201804, China



### ARTICLE INFO

**Keywords:**

Critical instantaneous decision events  
Trajectory data  
Permutation entropy  
Cube searching algorithm  
Mixed-flow intersections

### ABSTRACT

Mixed-flow intersections are prevailing in many developing countries such as China and India. At mixed-flow intersections, there is no clear lane discipline or regular trajectories within the intersection, especially for the non-motorized traffic. This leads to more interactions and encounters between the motorized traffic and the non-motorized traffic. Hence, critical instantaneous decision events such as abrupt accelerating, decelerating, jerking, swerving, and swinging, may occur more frequently, which result in potential traffic conflicts and crashes. This study presents a methodology to identify critical instantaneous decision events at the mixed-flow signalized intersections, based on the entropy theory and high-resolution vehicle trajectory data. A three-dimensional cube searching algorithm is firstly proposed to extract general traffic events by examining the proximity between trajectories. A novel model incorporating vehicle kinematics and Permutation Entropy is then developed to identify critical events, by quantifying driving volatility based on the time-serial trajectory data. Next, 3,349 vehicle trajectories and 805 bicycle trajectories with a resolution of 0.12 s collected at a signalized intersection in Shanghai are used to demonstrate the proposed method. Results show that the proposed method is capable of identifying critical instantaneous decision events, and tends to produce a higher identification ratio comparing with the conventional method solely based on kinematic thresholds. A sensitivity analysis is also conducted to investigate the effects of model parameters on the performance of the proposed method. The presented work could be applied for traffic safety assessment, real-time driving alert systems, and early diagnosis of risk-prone road users at mixed-flow intersections.

### 1. Introduction

Urban intersections are characterized by mixed traffic flow in numerous developing countries such as China and India. There is no clear lane discipline within the intersection, especially for non-motorized vehicles and turning motorized vehicles, as illustrated in Fig. 1 (Ma et al., 2017). Vehicle trajectories are fairly irregular and random due to the interference with each other (Fu et al., 2017; Ni et al., 2016). In this context, critical instantaneous decision events may occur more frequently, in which involved road users have to make decisions in a short time and perform evasive maneuvers with noticeable driving volatility (Wang et al., 2015). Typical critical decision events include abrupt accelerating, decelerating, jerking, swerving, and swinging. These events have been regarded as primary factors leading to traffic conflicts and crashes (World Health Organization, 2017; AASHTO, 2010). Hence, identifying critical instantaneous decision events can greatly contribute to the assessment of intersection safety and the development of safety improvement countermeasures.

Existing methods of identifying critical instantaneous decision events are mainly based on surrogate safety analysis (Gettman et al., 2008). A traffic event is often recognized as a critical event if its surrogate safety measures such as Post-Encroachment Time (PET) and Time-to-Collision (TTC) exceed certain pre-defined thresholds (AASHTO, 2010). The inputs of such analysis are generally two-dimensional (e.g. time-distance) vehicle trajectories, which are created by compositing the subject vehicle's lateral and longitudinal displacements into a generalized distance. The compositing treatment is generally fine with the regular vehicle trajectories but might neglect potential interactions and encounters among vehicles in the case of mixed traffic flow.

Recently, massive amounts of high-resolution trajectory data have become available, owing to the developments of connected vehicles, smartphone-based navigation, and video detection technologies. High-resolution trajectory data can not only provide rich and timely traffic flow information, but also capture small displacements of moving objects in the lateral and horizontal dimensions. Thus, trajectory-based traffic state estimation, signal control optimization, and traffic safety

\* Corresponding author.

E-mail address: [tang@tongji.edu.cn](mailto:tang@tongji.edu.cn) (K. Tang).



**Fig. 1.** Illustration of a mixed-flow intersection without clear lane discipline.

analysis have become feasible and promising (Kluger et al., 2016; Essa and Sayed, 2018).

In view of that, this study takes advantage of high-resolution trajectory data to identify critical instantaneous decision events, by extracting general events and quantifying driving volatility. Specifically, this paper develops a three-dimensional cube searching algorithm to recognize the proximity between trajectories in spatial and temporal dimensions. The algorithm can dynamically detect potential interacting zones without relying on a fixed observing site, which is thus capable of identifying the complicated interactions with evasive movements at mixed-flow intersections. Besides, the distribution of kinematic indicators is applied to pick up abnormal driving patterns with prompt braking, speeding, and steering. Then, Permutation Entropy (PE) of kinematic indicators is calculated to identify evasive maneuvers during traffic events, based on the complexity of time-serial trajectory data.

The remainder of this paper is organized as follows. Section 2 presents a literature review on the identification of safety critical events. Section 3 describes the methodology that extracts general traffic events and identifies critical instantaneous decision events. Section 4 introduces data collection and model calibrations. Section 5 presents sensitivity analysis of model parameters. Section 6 closes the paper with conclusions and further research.

## 2. Literature review

Trajectories crossing each other in an designated area during a given time interval were flagged as a traffic event (Ni et al., 2016). In particular, safety critical events were defined as “crashes or situations that requires a sudden, evasive manoeuvre to avoid a hazard or to correct for unsafe acts performed by the driver himself/herself or by other road users” (Bagdadi, 2013). The correlation between hazardous situations and crashes has been well demonstrated in previous studies (Wali et al., 2018; Ryder et al., 2018).

Recently, trajectory data collected in naturalistic driving studies or by video image processing has been utilized to identify safety critical events and risk-prone drivers. Studies based on naturalistic driving data along with questionnaires could evaluate relationships among driving environment, demographic characteristics and risky driving behavior (Bagdadi, 2013; Feng et al., 2017; Gershon et al., 2018). However, naturalistic driving data is hard to access for most researchers. While naturalistic driving studies primarily focused on motorized traffic, more studies based on video data investigated pedestrians and non-motorized traffic. The detection of safety critical events based on video data was achieved with different methods. One is to set certain threshold values for surrogate safety measures (Ismail et al., 2009; Tageldin et al., 2018). The other is to utilize the machine learning theory to improve accuracy

(Saunier and Sayed, 2007).

Proximity indicators as a sort of safety measures have been widely used for safety evaluation in past decades. The temporal and spatial proximity indicators were adopted to measure the similarities among road users by estimating the projected points of conflicts (Archer, 2005; Gettman et al., 2008; Lareshyn et al., 2010). However, potential traffic interactions might be neglected since vehicle trajectories are quite irregular in the mixed traffic flow conditions. Earlier studies showed that evasive action-based indicators were more probable to identify pedestrian conflicts in high mixed traffic environments than temporal proximity measures (Tageldin and Sayed, 2016; Tageldin et al., 2017).

Besides proximal safety indicators, the kinematics has been regarded as the key information describing driving behavior and vehicle performance. Acceleration and jerk were widely used as kinematic measures. Acceleration containing longitudinal and lateral acceleration was investigated in prior studies (Vlahogianni et al., 2014). Jerk also showed good performance in classifying driving events (Wang et al., 2015; Bagdadi and Várhelyi, 2011). Besides, multiple indicators were proposed, including the ratio of standard deviation to mean of acceleration, peak-to-peak jerk, drivers' frequencies of using large jerk, and so on (Langari and Won, 2005; Bagdadi and Várhelyi, 2013; Feng et al., 2017).

Nevertheless, no consensus existed regarding the thresholds of kinematic indicators in literature. The thresholds were previously determined by the 85% quartile (Lee and Jang, 2017), the 99.9% quartile (Feng et al., 2017), the mean plus/minus two standard deviations (Khattak et al., 2015), or other single threshold values. However, applying a single threshold value only represented the typical driving pattern in the local area without considering the individuality of road users and the performance of vehicles. To address the issue, the variation in acceleration and jerk at different speeds was explored and the points out of the mean plus/minus standard deviation band was reported as the “volatile” driving seconds (Wang et al., 2015).

Additionally, volatile driving time within indicator thresholds does not indicate a safety passage (Kluger et al., 2016). For instance, non-motorized vehicles snaking through mixed-flow intersections in changing directions can easily generate traffic safety hazards. Besides, a driver accelerating followed by braking repeatedly in a short time interval may also affect other drivers and lead to erroneous driving decisions. However, road users accelerate, brake, and steer frequently and normally at intersections. Controlled and powerful actions do not mean that the driver is in a risky encounter.

Therefore, this study aims to close the research gaps in the identification of critical instantaneous decision events. Trajectory proximities in spatial and temporal dimensions are firstly examined. Then, the boundaries to define driving variation at each speed group are investigated instead of using a single threshold value. To target critical events, driving volatility is further quantified by entropy based on time-serial trajectory data during interaction intervals.

## 3. Methodology

### 3.1. Variable declaration

Notations used in this paper are summarized in Table 1.

### 3.2. Extraction of general traffic events

Conventional trajectory-based methods to identify traffic events detect static zones, like a fixed grid, as potential conflict locations, as illustrated in Fig. 2a. Surrogate safety indicators are then calculated based on two-dimensional (e.g. time-distance) vehicle trajectories, which are created by compositing the subject vehicle's lateral and longitudinal displacements into a generalized distance, as illustrated in Fig. 2b. However, if road users perform evasive actions, for instance, changing lanes, the potential conflict zones are dynamic. To overcome

**Table 1**  
Notations.

Symbols	Definitions
$L$	The length of the space-time cube. (m)
$W$	The width of the space-time cube. (m)
$T$	The height of the space-time cube. (s)
$\vec{v}$	The resultant velocity. (m/s)
$\vec{v}_x$	The velocity in the x-direction. (m/s)
$\vec{v}_y$	The velocity in the y-direction. (m/s)
$(x, y)$	The point within the space-time cube.
$(x_n, y_n)$	The trajectory point at the time n.
$l_{01}$	The line through the trajectory point in the direction of $\vec{v}$ .
$l_{02}$	The line which is perpendicular to $\vec{v}$ and passes through the trajectory point.
$l_1, l_2, l_3, l_4$	Cube boundaries in the XY plane.
$t_n$	The time of the trajectory data point. (s)
$T_c$	The ceiling of the space-time cube. (s)
$T_f$	The floor of the space-time cube. (s)
$\Delta t$	The sampling interval. (s)
$\vec{a}$	Acceleration. ( $m/s^2$ )
$\vec{J}$	Jerk. ( $m/s^3$ )
$\vec{K}$	Curvature. (1/m)
$\vec{CR}$	The change rate of curvature. (1/m/s)
$m$	The embedding dimension.
$\tau$	The time delay.
$X'$	The reconstructed time series.
$\pi(i)$	The permutation type of the reconstructed row vector.
$f(\pi(i))$	Number of reconstructed row vectors that order in type $\pi(i)$ .
$\theta_1^+$	The mean plus standard deviation of positive indicator values.
$\theta_1^-$	The mean minus standard deviation of negative indicator values.
$\theta_2^+$	The mean plus two standard deviation using positive indicator values.
$\theta_2^-$	The mean minus two standard deviation using negative indicator values.
$\mu$	The average.
$\sigma$	The standard deviation.
$var$	The variance.

the weakness, this study proposes a three-dimensional method to dynamically identify general traffic events in mixed traffic flow, without assumptions of where and when interactions would happen, as illustrated in Fig. 2c. The proposed method also avoids multiple computations at each time-step.

In the proposed three-dimensional method, a space-time cube is firstly defined based on trajectories. Let the cube  $(L, W, T)$  denote a road user moving at segments and intersections. Each road user occupies part of the three-dimensional space for safety whose length is  $L$ , width is  $W$ , and height is  $T$ . If another road user is intruding into the cube, the subject is encountering a traffic event. The use of space-time cubes helps define distinct modes of transportation since road users need various space and time to ensure safety. A road user passing through an intersection is defined as either a general traffic event or an undisturbed passage. Three main steps of the algorithm are described in the remainder of this section.

### 3.2.1. Step 1: building the space-time cube of each road user

The first step is to build the space-time cube according to the mode of transportation and the direction of motion. In the spatial dimension, the typical sizes of road users are used as the sizes of corresponding cubes. Sizes of cubes are presented in model calibration. To describe the orientation of cubes, linear programming is applied. Thus, the zone of cubes in the XY plane is defined in three scenarios.

As shown in Fig. 3, let  $\vec{v}$  denote resultant velocity. The road user is traveling at the speed  $\vec{v}_x$  in the x-direction and the speed  $\vec{v}_y$  in the y-direction. Besides, let  $(x, y)$  denote any point within the cube and  $(x_n, y_n)$  denote the trajectory point. Let  $l_{01}$  and  $l_{02}$  denote lines through the trajectory point  $(x_n, y_n)$ ;  $l_{01}$  is in the direction of  $\vec{v}$ , and  $l_{02}$  is

perpendicular to  $\vec{v}$ . Additionally,  $l_1, l_2, l_3$ , and  $l_4$  are cube boundaries in the XY plane.

#### Scenario 1: the road user is moving in the x/y direction

When the road user is moving in the x-direction (shown in Fig. 3a), points in the cube are described by the following equations:

$$\begin{cases} x_n - \frac{L}{2} \leq x \leq x_n + \frac{L}{2} \\ y_n - \frac{W}{2} \leq y \leq y_n + \frac{W}{2} \end{cases} \quad (1)$$

When the road user is moving in the y-direction (shown in Fig. 3b), points in the cube are described by the following equations:

$$\begin{cases} x_n - \frac{W}{2} \leq x \leq x_n + \frac{W}{2} \\ y_n - \frac{L}{2} \leq y \leq y_n + \frac{L}{2} \end{cases} \quad (2)$$

#### Scenario 2: the road user is moving towards the first or the third quadrant

If a road user is moving towards the first quadrant, as shown in Fig. 3c, the equation of  $l_{01}$  is set up as follows:

$$y - y_n = \frac{v_y}{v_x}(x - x_n) \quad (3)$$

In the vertical direction, the equation of  $l_{02}$  is established:

$$y - y_n = -\frac{v_y}{v_x}(x - x_n) \quad (4)$$

According to the difference of y-intercepts between  $l_1$  and  $l_{01}$ , the equation of  $l_1$  is:

$$y - y_n = \frac{v_y}{v_x}(x - x_n) + \frac{W\sqrt{v_y^2 + v_x^2}}{2v_x} \quad (5)$$

Similarly, equations of  $l_3, l_2$ , and  $l_4$  are known. Therefore, the zone of cube in the XY plane is expressed as:

$$y - y_n \leq \frac{v_y}{v_x}(x - x_n) + \left| \frac{W\sqrt{v_y^2 + v_x^2}}{2v_x} \right| \quad (6-1)$$

$$y - y_n \leq -\frac{v_x}{v_y}\left(x - x_n - \left| \frac{L\sqrt{v_y^2 + v_x^2}}{2v_x} \right| \right) \quad (6-2)$$

$$y - y_n \geq \frac{v_y}{v_x}(x - x_n) - \left| \frac{W\sqrt{v_y^2 + v_x^2}}{2v_x} \right| \quad (6-3)$$

$$y - y_n \geq -\frac{v_x}{v_y}\left(x - x_n + \left| \frac{L\sqrt{v_y^2 + v_x^2}}{2v_x} \right| \right) \quad (6-4)$$

#### Scenario 3: the road user is moving towards the second or the fourth quadrant

Points in the XY plane within a cube are expressed like Eq. (6) in form. Yet the left part should be greater than or equal to the right part in Eq. (6-2), and the value on the left should be less than or equal to the value on the right in Eq. (6-4).

As for the temporal dimension, PET is chosen as the measure of cubes. Unlike TTC and some other indicators, PET removes the assumptions of moving path and constant speed, which makes it more practical in the application. The ranges of cubes are defined by Eqs. (7) and (8) in the temporal dimension, where  $t_n$  denotes the time of the trajectory data point,  $T_c$  is the ceiling of the cube, and  $T_f$  is the floor of the cube. Hence, the space-time cube for each mode of transportation is defined.

$$T_c = t_n + \frac{1}{2}T \quad (7)$$

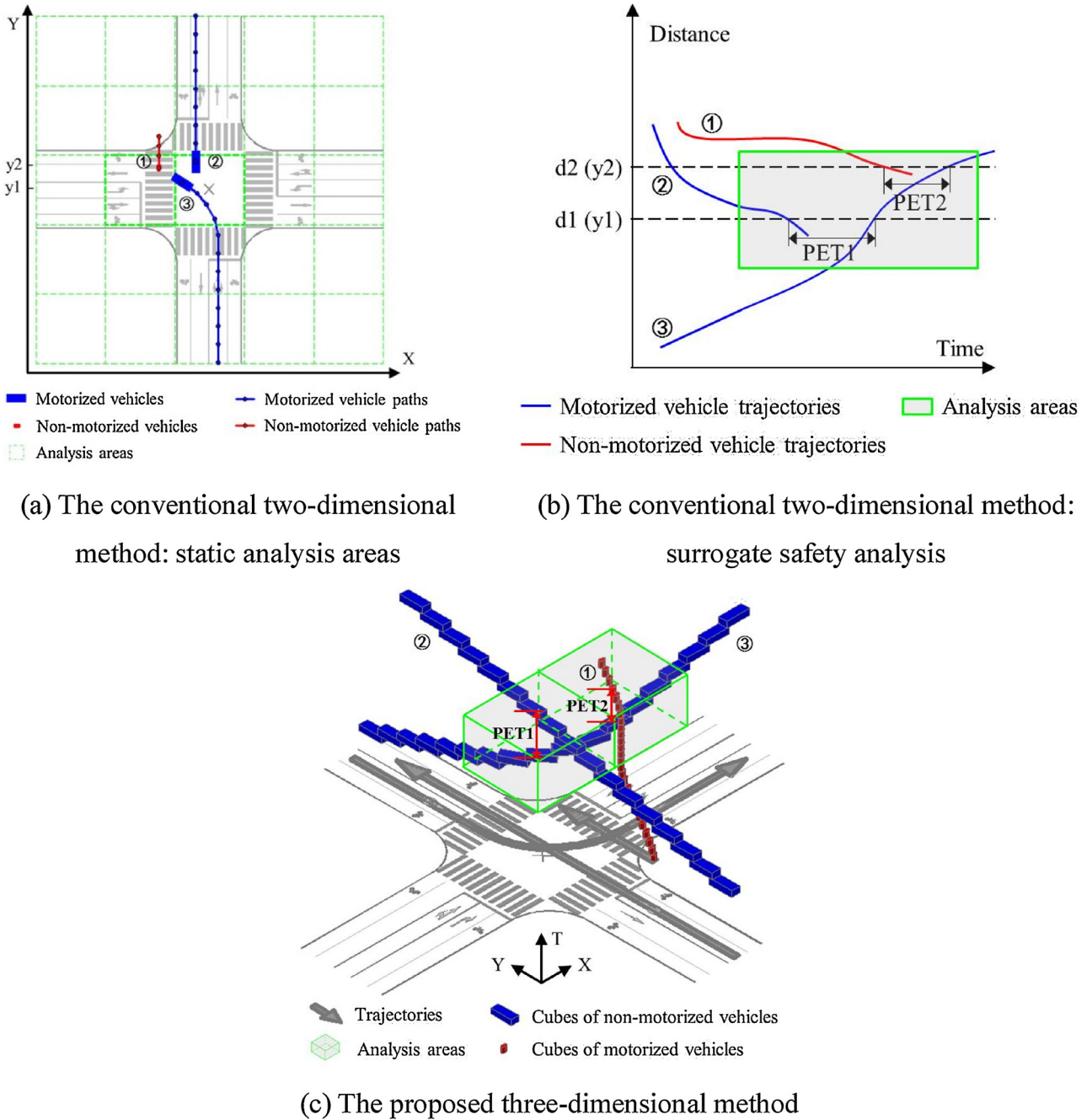


Fig. 2. Comparison of the conventional two-dimensional method and the proposed three-dimensional method.

$$T_f = t_n - \frac{1}{2}T \quad (8)$$

### 3.2.2. Step 2: sliding the cube for each trajectory

For each type of road user, the size and the shape of the space-time cube are determinate. The cube is built at each time step from the very beginning of the movement, sliding along the trajectory, as shown in Fig. 2c. It is noted that the cubes are not standing side by side but overlapping because the time step is tiny. The sliding cube forms a pipeline representing the potential interacting time and zones according to the mode of transportation in the three-dimensional space.

### 3.2.3. Step 3: examining general traffic events

Vehicles need space and time resources of the traffic system to pass safely. The space-time cube represents the occupied resource by a road

user at a time. If the cube is encroached by other objects, the road user is uncomfortable or endangered. Therefore, the algorithm checks whether the three-dimensional cube contains trajectory points of other objects at each time step. The event is recorded, and the minimum PET is saved since a group of road users may encounter more than once.

Identification results are randomly selected for verification. Firstly, trajectory data points in an event are extracted to confirm that those points are within a risky distance and time interval of a space-time cube. Secondly, identification results are checked by video observation. Final results are prepared for the identification of critical instantaneous decision events.

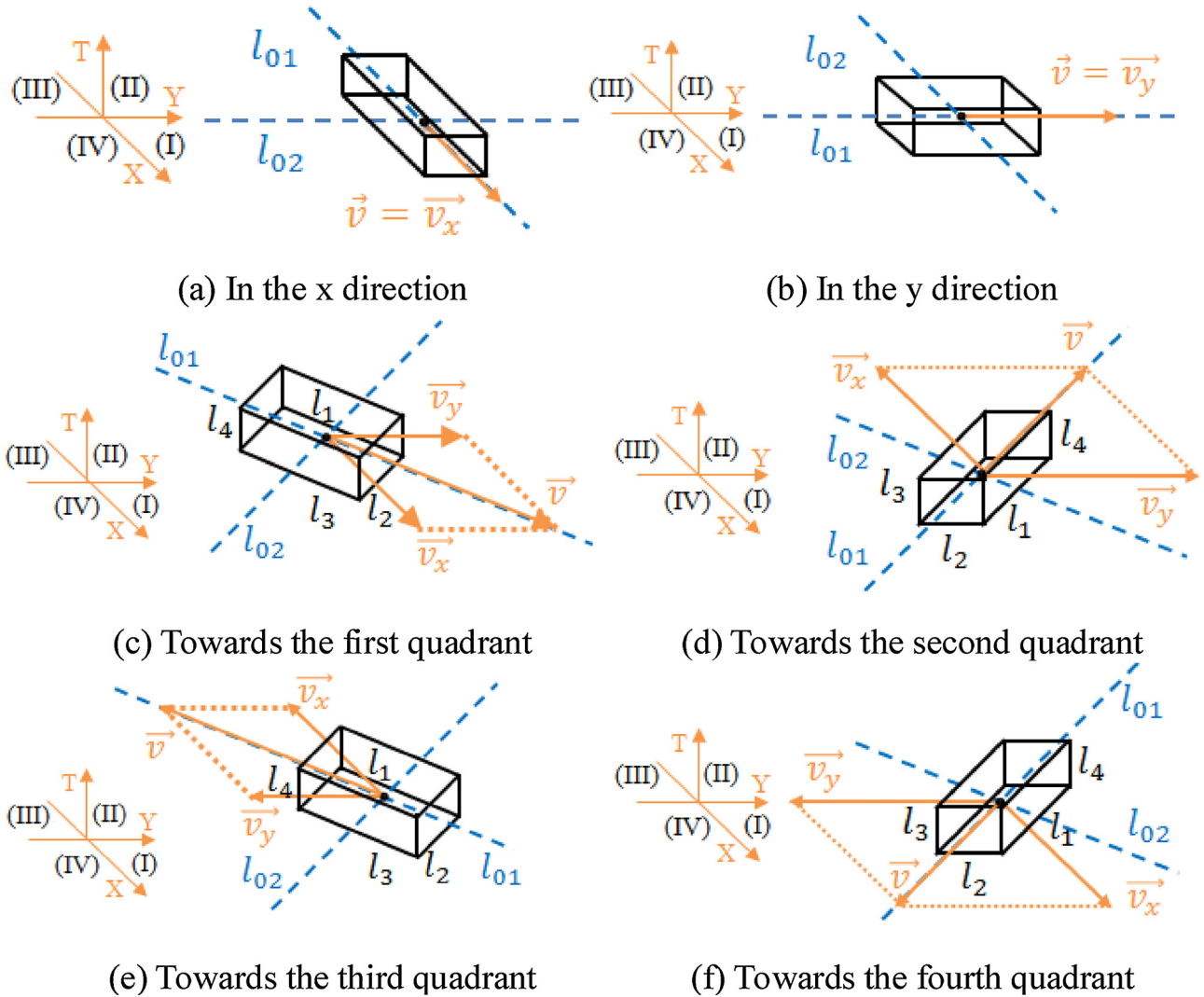


Fig. 3. Three-dimensional cubes.

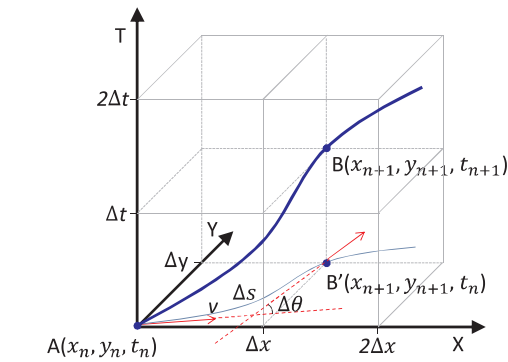


Fig. 4. Calculating kinematic indicators.

### 3.3. Identification of critical instantaneous decision events

#### 3.3.1. Extracting time subsequences with events

Time subsequences are extracted, centering around the time of minimum PET. Time intervals before and after the time are analyzed because it is uncertain when the involved road user will make critical decisions to react. In this way, the changing process of the driver behavior is known, contributing to providing driver assistance advice effectively. If the trajectory time series of single road users is divided

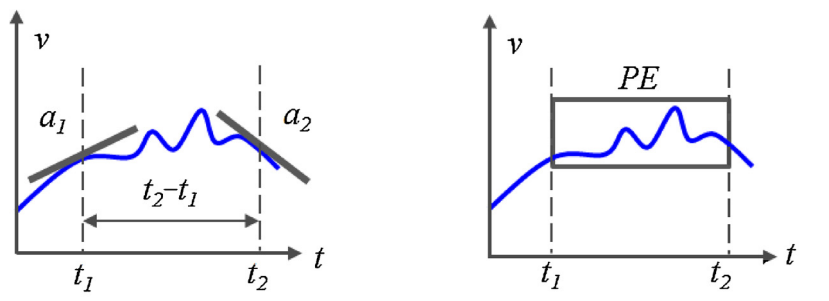
equally without considering the interacting time, an event may span multiple time windows. In that case, the time of instantaneous decision events could not be found accurately, and the change of driver behavior would be uncertain. Furthermore, choosing the length of time subsequences should consider the driver's reaction time and the data sampling rate. All the time subsequences are extracted with the same length for ease of later calculations.

#### 3.3.2. Recognizing abnormal driving time by the kinematic indicator distribution

Variations of the speed or direction can be observed when the driver takes evasive actions. Abnormal driving time occurs when the driving variation is beyond acceptable limits. Hence, the kinematic indicator distribution is applied to the time subsequence to filter normal driving time. Indicators include acceleration, jerk, curvature, and the change rate of curvature, characterizing the speeding behavior and the turning behavior. All the indicators at the time  $n$  can be calculated based on trajectory data, as illustrated in Fig. 4.

Let  $(x_n, y_n)$  denote the trajectory point at the time  $n$ ,  $(x_{n+1}, y_{n+1})$  denote the trajectory point at the next time step, and  $\Delta t$  denote the sampling interval. The resultant velocity  $\vec{v}$  is calculated, which is in the direction of  $\arctan \frac{v_y}{v_x}$ .

$$\vec{v}_x = \frac{dx}{dt} \quad (9)$$



(a) Acceleration for a time step      (b) Permutation Entropy for a time window

Fig. 5. Comparison of acceleration and permutation entropy.

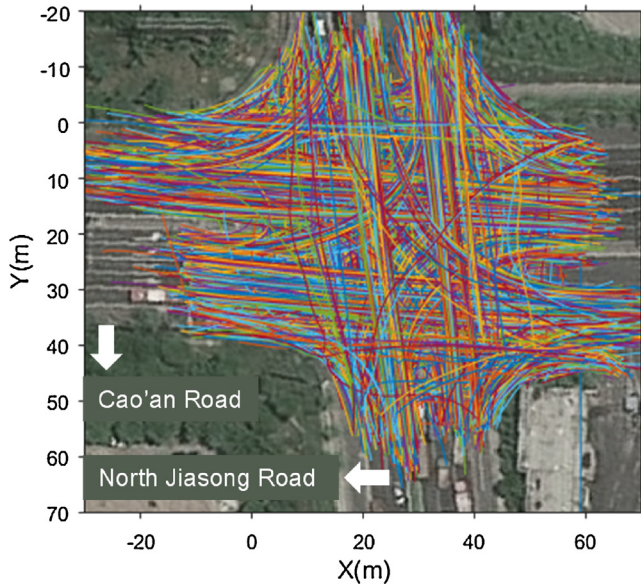


Fig. 6. Observed trajectories at the study intersection.

$$\vec{v}_y = \frac{d\vec{y}}{dt}$$

$$v = \sqrt{v_x^2 + v_y^2} = \sqrt{\left(\frac{x_{n+1} - x_n}{\Delta t}\right)^2 + \left(\frac{y_{n+1} - y_n}{\Delta t}\right)^2}$$

Acceleration  $\vec{a}$  is the rate of change of velocity  $\vec{v}$  with respect to time  $t$ . Positive acceleration represents that the vehicle is speeding up, and negative acceleration indicates that the road user is slowing down.

$$\vec{a} = \frac{d\vec{v}}{dt}$$

Jerk  $\vec{j}$  is the second derivative of velocity, representing the road user performing abrupt speeding or braking. Jerk is positive in the following cases: 1) braking more softly, 2) accelerating more forcefully, 3) decelerating and then accelerating. Otherwise, jerk can be negative or zero.

$$\vec{j} = \frac{d\vec{a}}{dt} = \frac{d^2\vec{v}}{d^2t}$$

Curvature  $\vec{k}$  is defined as the result of tangent angle  $\theta$  divided by the arc length  $s$ , as shown in Eq. (14). If the vehicle performs a sharp turn, the magnitude of curvature is large. Curvature is positive when the road user makes a right turn. Conversely, the curvature is negative.

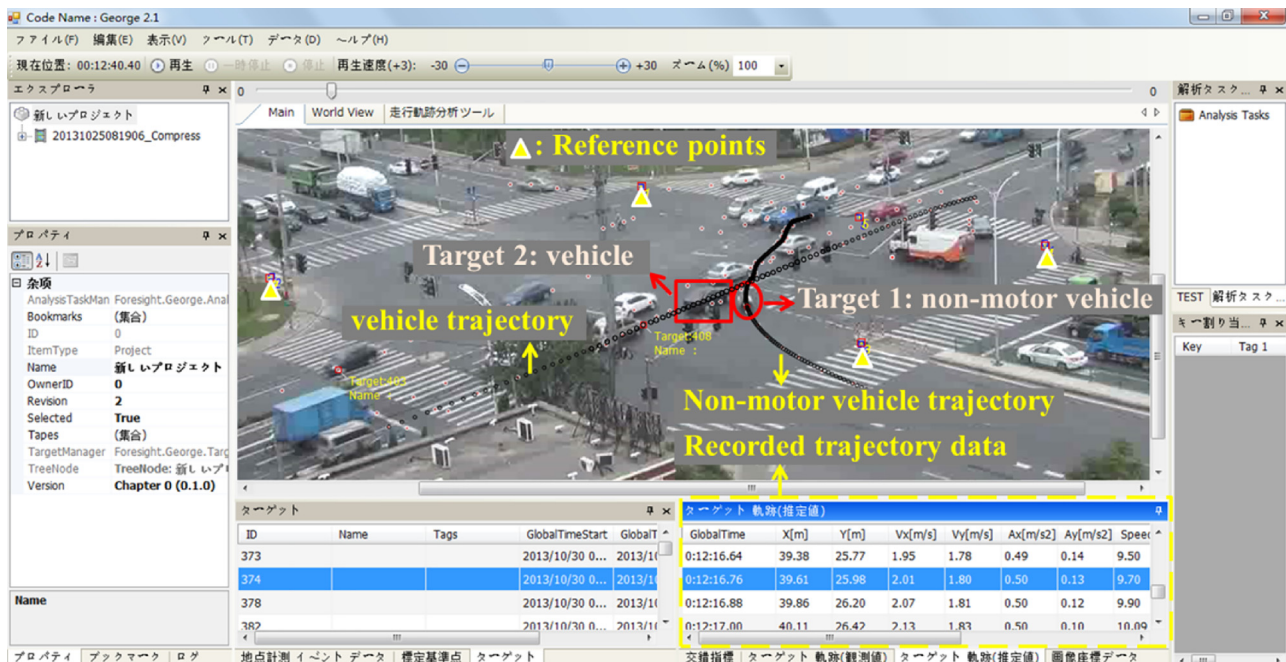


Fig. 7. Image-processing software used for extracting trajectories.

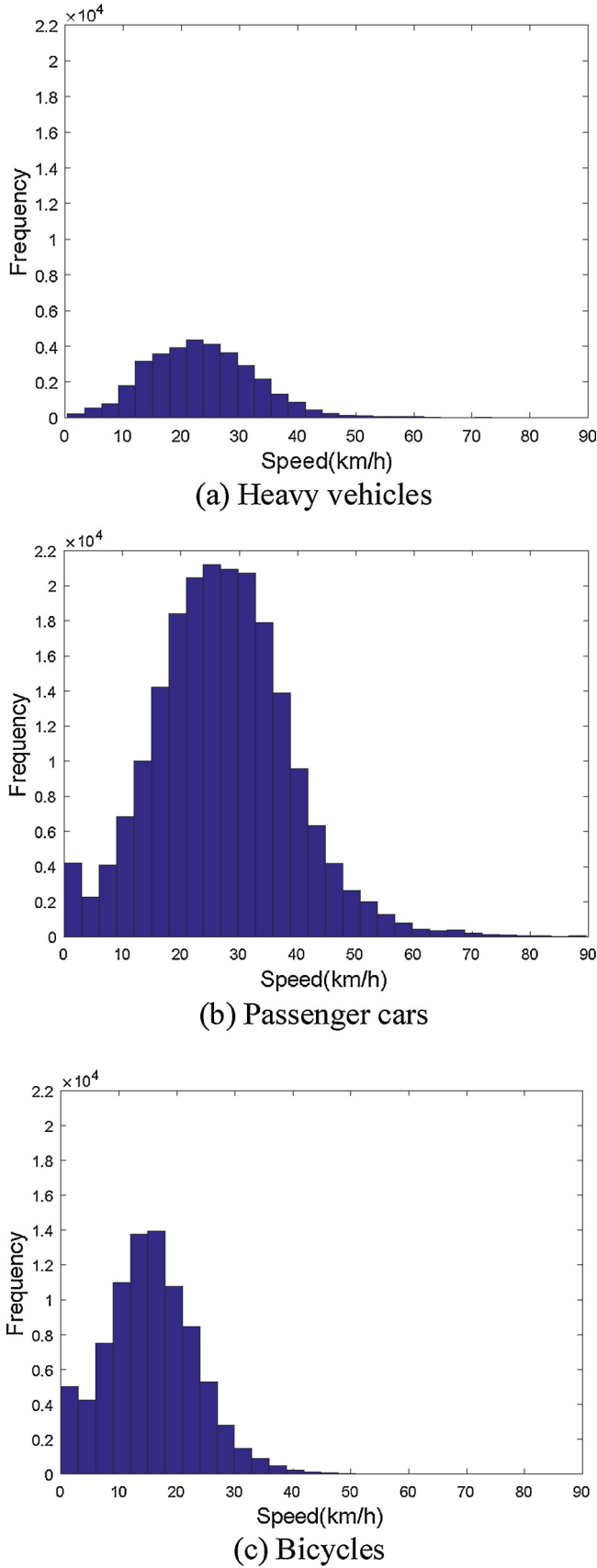


Fig. 8. Frequencies of trajectory data points at each speed group.

$$\vec{K} = \frac{d\vec{\theta}}{ds} \quad (14)$$

The change rate of curvature with respect to time,  $\vec{CR}$ , is calculated as Eq. (15).  $\vec{CR}$  represents the road user making a turn quickly or slowly. The positive or negative sign of  $\vec{CR}$  is consistent with curvature.

$$\vec{CR} = \frac{d^2\vec{\theta}}{dsdt} \quad (15)$$

### 3.3.3. Identifying critical instantaneous decision events by Permutation Entropy

Based on the typical driving pattern captured by the kinematic indicator distribution, driving fluctuations or complexities of trajectory time subsequences are analyzed. Permutation Entropy, drawing on the concept of information entropy, is standout among complexity measures of time series due to its robustness, simplicity, and low cost for calculation (Bandt and Pompe, 2002).

Generally, PE is comparative with acceleration in the field of traffic engineering. Firstly, while the acceleration is the change rate of resultant velocity, PE measures the saltation of speed if taking the series of resultant velocity as input data. Secondly, the acceleration is based on point-in-time, yet the PE is based on time frames or events. To examine the volatility of speed, the acceleration method calculates the difference between values at a given time step, while the PE method uses data in a time window without loss of information, as shown in Fig. 5.

To calculate the PE, the time series  $x = [x(1), x(2), \dots, x(N + (m - 1)\tau)]$  is firstly reconstructed as follows. It is noted that  $x$  can be  $a$ ,  $J$ ,  $K$ , or  $CR$ .

$$X' = \begin{bmatrix} x(1) & x(1 + \tau) & \dots & x(1 + (m - 1)\tau) \\ \vdots & \vdots & & \vdots \\ x(j) & x(j + \tau) & \dots & x(j + (m - 1)\tau) \\ \vdots & \vdots & & \vdots \\ x(N) & x(N + \tau) & \dots & x(N + (m - 1)\tau) \end{bmatrix} \quad (16)$$

Where,  $m$  represents the embedding dimension,  $\tau$  is the time delay, and  $X' = [X'(1), X'(2), \dots, X'(j), \dots, X'(N)]$  ( $j = 1, 2, \dots, N$ ) denotes the reconstructed time series.

For the reconstructed row vector  $X'(j)$ , elements are compared. The permutation type is defined as  $\pi(i)$ , where the potential  $\pi(i)$  ranges from 0 to  $m!$ . For example, the order type of [2, 7, 9] is 012 and the type of [7, 2, 9] is 102. Then, the relative frequency of  $\pi(i)$  is defined as:

$$p(\pi_i) = \frac{f(\pi(i))}{N} \quad (17)$$

Where,  $f(\pi(i))$  denotes number of  $X'(j)$  ( $j = 1, 2, \dots, N$ ) that orders in type  $\pi(i)$ . Further, Permutation Entropy (PE) is expressed as:

$$PE(x) = - \sum_{i=1}^{m!} p(\pi_i) \log [p(\pi_i)] \quad (18)$$

The PE of acceleration, jerk, curvature, and the change rate of curvature is calculated based on the above process. Finally, critical instantaneous decision events are identified if kinematic indicators reflecting extreme driving behavior or driving volatility are picked out by PE during an interaction interval.

## 4. Data description and model calibration

### 4.1. Data description

The study area is a four-leg signalized intersection between Cao'an Road and North Jiasong Road in Shanghai, China. The intersection was chosen because heavy vehicles (including trucks and buses), passenger cars, e-bikes, bicycles, and pedestrians share the traffic facilities, and

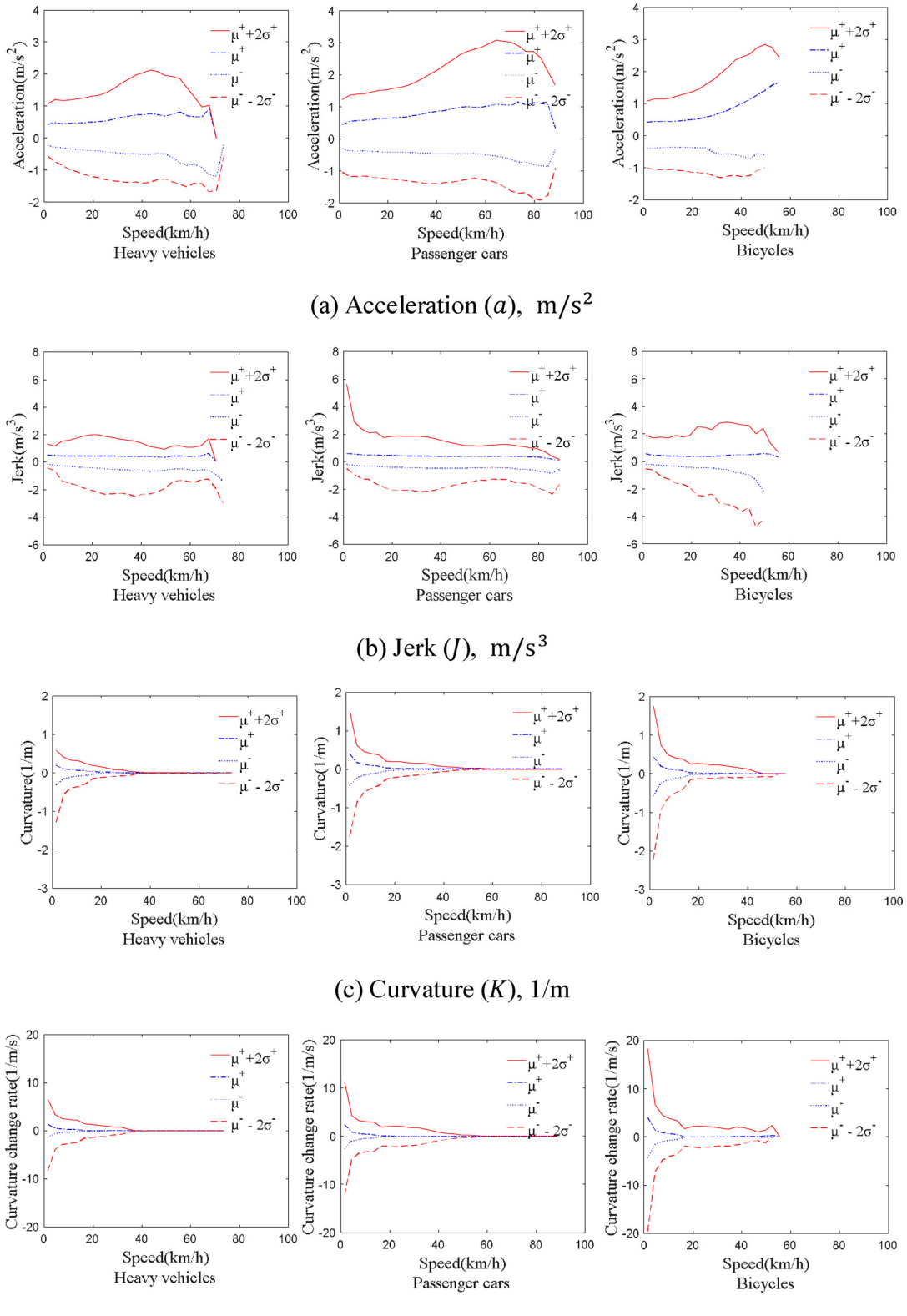


Fig. 9. Distribution of indicators for different vehicle types.

the road users are unruly to some extent. The majority of left-turning non-motorized vehicles went through the intersection by the means of twice crossing, while others traveled with motorized vehicles. Moreover, right-turning vehicles were free of signal control. Thus, there was a high possibility that critical instantaneous decision events could

be observed. The video was recorded during a morning peak on a workday. In the collected video data, a total of 419 heavy vehicles, 2930 passenger cars, and 805 bicycles were observed, and their trajectories are visualized in Fig. 6.

The trajectory data was extracted by a semi-automatic software, as

**Table 2**

Comparisons of the conventional method and the proposed method.

	V (veh)	NT	Thr	The conventional method		The proposed method		Difference ([2]-[1])
				NC	P[1]	NC	P[2]	
Heavy vehicles	419	143	1	28	19.7%	41	28.9%	9.2%
			2	8	5.6%	25	17.6%	12.0%
Passenger cars	2930	1390	1	539	38.8%	676	48.6%	9.9%
			2	391	28.1%	567	40.8%	12.7%
Bicycles	805	357	1	79	22.1%	125	35.0%	12.9%
			2	64	17.9%	114	31.9%	14.0%
All vehicles	4154	1890	1	646	26.9%	842	37.5%	10.6%
			2	463	17.2%	706	30.1%	12.9%
			Mean	555	22.1%	774	33.8%	11.7%

Note: V denotes volumes. NT denotes number of total decision events. Thr = 1 means  $\theta_1^+$  and  $\theta_1^-$ . Thr = 2 means  $\theta_2^+$  and  $\theta_2^-$ . NC denotes number of critical instantaneous decision events. P denotes the proportion.

presented in Fig. 7 (Suzuki and Nakamura, 2006). To begin with, global coordinates of at least three reference points in the image were input to calibrate the video coordinates until the accuracy met the requirement. Then, road users were tracked by manually clicking a fixed position of their bodies every 0.12 s, for example, the waists of riders and the right front wheels of motorized vehicles. Kalman smoothing algorithm was then applied to process the clicked paths. In this study, only the trajectories inside the intersection were recorded and used in the analysis.

#### 4.2. Model calibration

Parameter settings are presented here to adapt to the collected data. Based on field observation and validation on videos, 1.5 s is applied to the height of space-time cubes (i.e.  $T$ ). Sizes of cubes in the XY plane refer to typical vehicles: 8.5 m × 2.5 m for heavy vehicles, 4.5 m × 1.8 m for passenger cars, and 1.7 m × 0.7 m for non-motorized vehicles. When extracting traffic events, the specific value of 3 s is chosen as the length of time subsequences, notably 1.5 s before and 1.5 s after the interacting time, to make sure that the time interval is capable for road users to make decisions (Bagdadi and Várhelyi, 2013). Additionally, trajectory data is divided into groups depending on speeds. The group interval is 3 km/h, and the sample size of each speed group is presented in Fig. 8.

The distribution of kinematic indicators is built to identify critical driving behavior. Indicators used in this study are acceleration, jerk, curvature, and the change rate of curvature. The boundaries of these indicators are defined as follows (Wang et al., 2015; Khattak et al., 2015):

$$\theta_1^+ = \mu^+ + \sigma^+ \quad (19-1)$$

$$\theta_1^- = \mu^- - \sigma^- \quad (19-2)$$

$$\theta_2^+ = \mu^+ + 2\sigma^+ \quad (20-1)$$

$$\theta_2^- = \mu^- - 2\sigma^- \quad (20-2)$$

where  $\theta_1^+$  denotes the mean plus standard deviation of positive indicator values,  $\theta_1^-$  is the mean minus standard deviation of negative indicator values,  $\theta_2^+$  denotes the mean plus two standard deviation using positive indicator values,  $\theta_2^-$  is the mean minus two standard deviation using negative indicator values,  $\mu$  represents the average, and  $\sigma$  denotes the standard deviation.

Thresholds can be further adjusted according to the study area and research conditions. Besides, moving average method is applied to smooth the band boundaries. The distribution using  $\theta_2^+$  and  $\theta_2^-$  is presented in Fig. 9 to show the extreme driving behavior.

Fig. 9 indicates that driving behavior and vehicle performance vary from road user types and driving conditions, and the upper band and the lower band are not symmetrical. It reveals that driving behavior is distinct when accelerating, decelerating and turning. Besides, the

ability to swerve a vehicle declines at higher speeds. Heavy vehicles are hard to perform a sharp turn comparing with passenger cars. Non-motorized vehicles are the most flexible type for steering. However, their variable trajectories easily generate risky driving decisions.

Furthermore,  $\mu + 2\text{var}$  is used for PE thresholds, where  $\text{var}$  denotes the variance. In the PE algorithm, the embedding dimension  $m$  is the critical parameter, which affects the reconstructed matrix and computation time. In this study,  $m = 4$  and  $\tau = 4$ , which are discussed in the sensitivity analysis.

## 5. Results and discussion

### 5.1. Comparisons with the conventional method

Road users involved in general traffic events are supposed to have made driving decisions. Results of the three-dimensional cube searching algorithm are compared with traffic interactions identified by a human observer, according to the FHWA manual (Parker and Zegeer, 1989). A unified height of space-time cubes for different types of road users, i.e. 1.5 s, could enable the algorithm to automatically capture 82.5% of general traffic events, while detecting 41.5% of undisturbed passages as general traffic events. After adjusting the heights of space-time cubes, i.e. 1.5 s for heavy vehicles, 1.2 s for passenger cars and 1.0 s for bicycles, the false positive rate falls to be 29.3% while the true positive rate reduces to be 66.2%. Those mismatching might be caused by the errors in vehicle tracking, improper sizes of space-time cubes, and the errors in observing driving decision events by the evasive action-based methods.

Furthermore, results of the proposed method are compared with a conventional method that applies dynamic threshold bands of kinematic indicators to identify critical instantaneous decision events, as shown in Table 2 (Wang et al., 2015; Khattak et al., 2015). It is noted that besides acceleration and jerk, curvature and the change rate of curvature are also analyzed in the conventional method. On average, 22.1% of total decision events are identified as critical instantaneous decision events by the conventional method, while the recognition rate of the proposed method is 33.8%.

The identification results are reasonable for the following reasons. Road users move at relatively small headway at intersections. Noticeable driving variation probably affects other road users and causes risky driving decisions. Accordingly, solely comparing kinematic indicators with the limits of vehicle capabilities may neglect some critical circumstances. Measuring volatility of time-serial trajectory data is another proper way to identify critical instantaneous decision events at intersections. To conclude, a key advantage of the proposed method over the conventional method is that traffic interactions and behavioral characteristics of individual road users are considered in the algorithm, contributing to a more practical identification result.

Fig. 10 demonstrates four cases of critical instantaneous decision

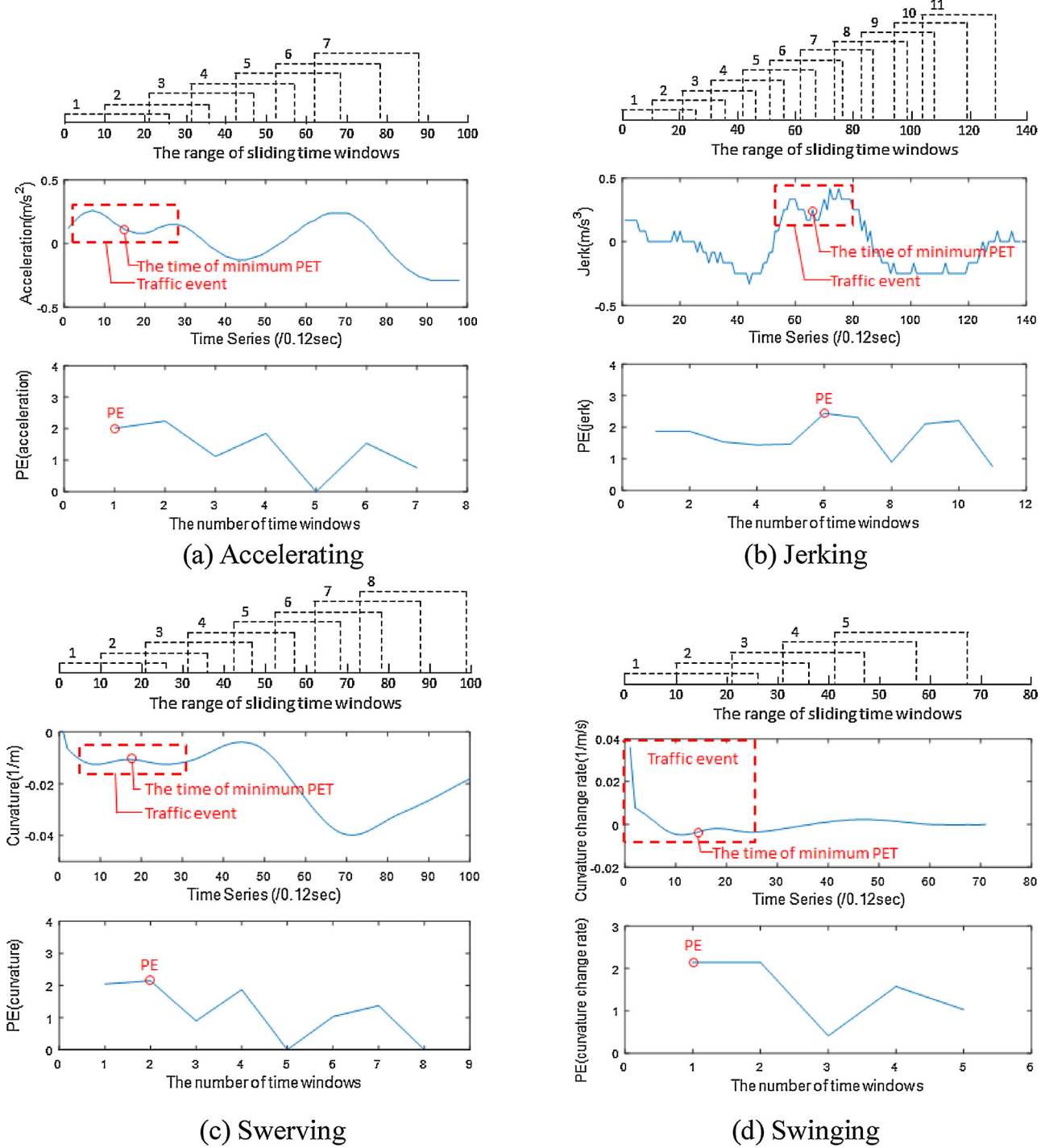


Fig. 10. Cases of critical instantaneous decision events.

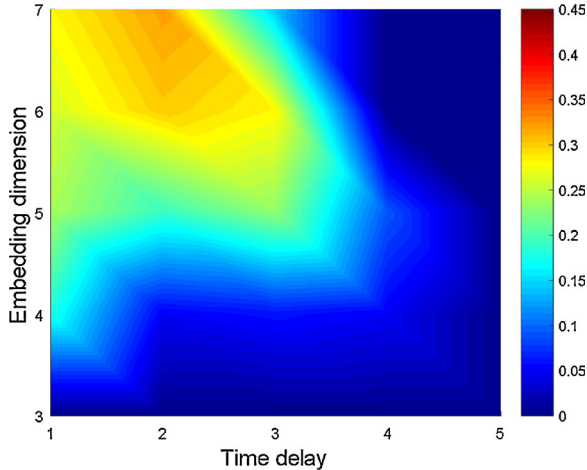
events including accelerating, jerking, swerving and swinging. The time frame is primarily identified as a general event. To show the PE results, PE is calculated with sliding time windows whose lengths are equal to the analyzed time frame's. In the following cases, although the kinematic indicator is not outside the threshold band at that speed group, once the driving volatility is identified by PE results, the traffic event is flagged as a critical instantaneous decision event.

As shown in Fig. 10a, the rider tended to accelerate successively when interacted with others. Fig. 10b shows two spikes of  $J$  during the event, indicating that the driver made a critical decision of jerking. As presented in Fig. 10c, the rider interrupted the process of turning when encountering other road users, and continued to make turns after

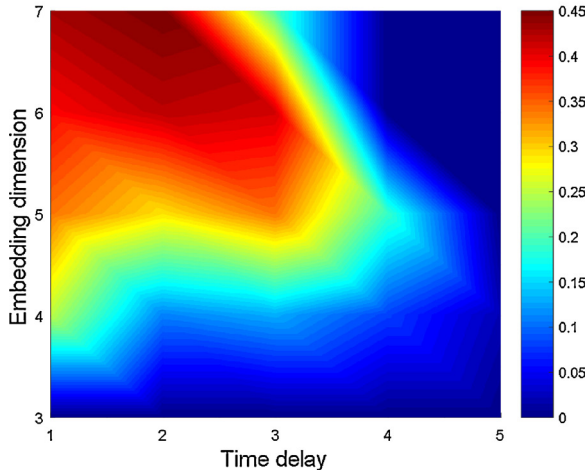
passing by. Fig. 10d shows  $CR$  changing from positive to negative in the event. Besides, the absolute value of  $CR$  has an evident downtrend and then rises and decreases gradually. This indicates that the driver made a decision to change direction very quickly to avoid a traffic conflict.

### 5.2. Sensitivity analysis

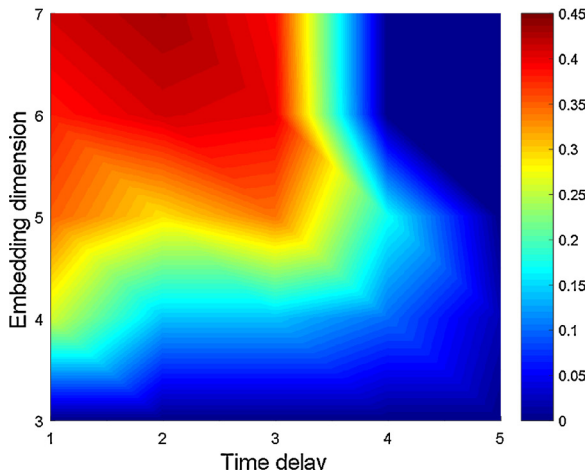
A sensitivity analysis is conducted in order to find appropriate values for the model parameters. Twenty-five scenarios are tested, with the embedding dimension ranging from 3 to 7 and the time delay ranging from 1 to 5 (Bandt and Pompe, 2002). If the PE value exceeds the threshold, the time subsequence is flagged as a volatile driving



(a) Heavy vehicles



(b) Passenger cars

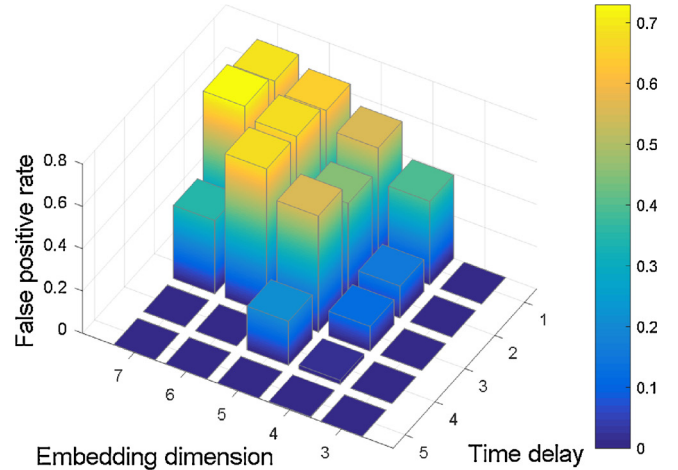


(c) Bicycles

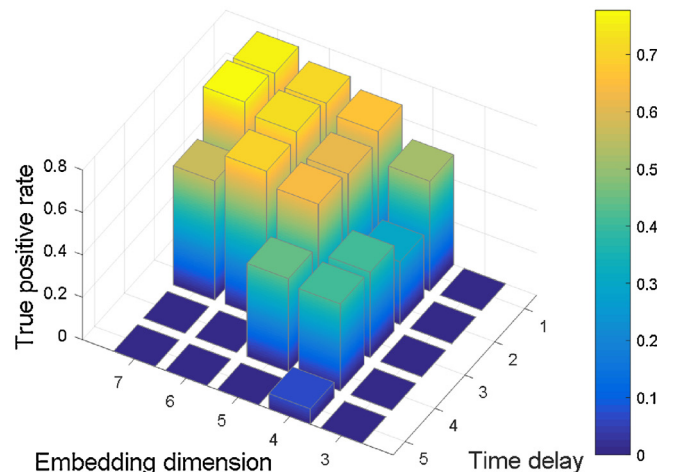
**Fig. 11.** The proportion of volatile driving events.

event. Otherwise, it is a normal driving event. The proportion of volatile driving events is recorded, as presented in Fig.11.

On the other hand, driving variation is observed by plotting the



(a) False positive rates



(b) True positive rates

**Fig. 12.** Sensitivity analysis of Permutation Entropy parameters.

speed diagram and the curvature diagram. Then, the PE results are compared with the real observations. False and true positive rates are calculated under different parameter settings, as shown in Fig. 12.

There are up to  $m!$  potentially ordinal patterns for elements of a reconstructed vector in the PE algorithm. If  $m$  is too low, the number of accessible permutation patterns will be small, and the result of PE will probably be unreliable. Besides, it is necessary that  $m! \ll N + (m - 1)\tau$  to achieve a reliable statistics (Kowalski et al., 2007; Li et al., 2014). However, if  $m$  is too high, the statistical condition may not be satisfied since motorized vehicles can take a short time to go through intersections, and the length of time series  $N + (m - 1)\tau$  is short. The increase of embedding dimension also brings longer calculation time since the size of the reconstructed matrix becomes bigger. Thus, it is efficient to choose a relatively small value of embedding dimension. Furthermore, the analysis shows that the PE algorithm captures 44.0% volatile driving events while it misclassifies 1.9% normal driving events as volatile driving events when  $m = 4$  and  $\tau = 4$ . When the embedding dimension and the time delay increase, the number of events exceeding the PE threshold rises, and both of the false positive rate and the true positive rate grow. The reason is that the reconstructed row vector  $x^r(j)$

picks trajectory data points at a large time step, releasing motion constraints and resulting in a messy order. Hence,  $m = 4$  and  $\tau = 4$  are chosen as the parameter setting in this case.

## 6. Conclusions

This paper presents a methodology to identify critical instantaneous decision events based on entropy theory using high-resolution trajectory data. The proposed method is verified in comparison with real observations and a conventional method. The presented work could be applied for traffic safety assessment, real-time driving alert systems, and early diagnosis of risk-prone road users at mixed-flow intersections.

Major contributions of this paper can be summarized below. Firstly, a three-dimensional analytical method is developed to dynamically identify traffic events with interactions, removing constraints of fixed-zone detections and multiple computations at each time-step. Secondly, the driving variation is evaluated from not only regional but also individual behavioral aspects by the kinematic indicator distribution and PE, respectively. The PE measures driving volatility by quantifying the complexity of time-serial trajectory data.

Future directions of the presented work are summarized as follows. Firstly, real traffic accident data can be used to further calibrate the model parameters and validate the proposed method. Secondly, the applicability of the proposed method needs to be comprehensively investigated, by considering various intersection types, signal control schemes, and compositions of traffic flow, etc. Thirdly, it is also interesting to integrate the proposed method with naturalistic driving data or driving simulation data.

## Acknowledgements

This study was supported by the National Natural Science Foundation of China (No. 51208380). The authors would like to thank Prof. Hideki Nakamura from Nagoya University for providing the video analysis software.

## References

- AASHTO, 2010. Highway Safety Manual. American Association of State Highway and Transportation Officials, Washington, DC.
- Archer, J., 2005. Indicators for Traffic Safety Assessment and Prediction and Their Application in Micro-simulation Modelling: A Study of Urban and Suburban Intersections Dissertation. Lund University.
- Bagdadi, O., 2013. Assessing safety critical braking events in naturalistic driving studies. *Transp. Res. Pt. F* 16, 117–126.
- Bagdadi, O., Várhelyi, A., 2011. Jerky driving—an indicator of accident proneness? *Accid. Anal. Prev.* 43 (4), 1359–1363.
- Bagdadi, O., Várhelyi, A., 2013. Development of a method for detecting jerks in safety critical events. *Accid. Anal. Prev.* 50 (2), 83–91.
- Bandt, C., Pompe, B., 2002. Permutation entropy: a natural complexity measure for time series. *Phys. Rev. Lett.* 88 (17), 174102.
- Essa, M., Sayed, T., 2018. Traffic conflict models to evaluate the safety of signalized intersections at the cycle level. *Transp. Res. C* 89, 289–302.
- Feng, F., Bao, S., Sayer, J.R., Flannagan, C., Manser, M., Wunderlich, R., 2017. Can vehicle longitudinal jerk be used to identify aggressive drivers? An examination using naturalistic driving data. *Accid. Anal. Prev.* 104, 125–136.
- Fu, T., Mirandamoreno, L., Saunier, N., 2017. A novel framework to evaluate pedestrian safety at non-signalized locations. *Accid. Anal. Prev.* 111 (2), 23–33.
- Getman, D., Sayed, T., Pu, L., Shelby, S., 2008. Surrogate Safety Assessment Model and Validation. FHWA-HRT-08-051. Federal Highway Administration. U.S. Department of Transportation, Washington, D.C.
- Gershon, P., Ehsani, J., Zhu, C., O'Brien, F., Klauer, S., Dingus, T., Simons-Morton, B., 2018. Vehicle ownership and other predictors of teenagers' risky driving behavior: evidence from a naturalistic driving study. *Accid. Anal. Prev.* 118, 96–101.
- Ismail, K., Sayed, T., Saunier, N., Lim, C., 2009. Automated analysis of pedestrian-vehicle conflicts using video data. *Transp. Res. Rec. J. Transp. Res. Board* 2140 (2140), 44–54.
- Khattak, A.J., Liu, J., Wang, X., 2015. Supporting instantaneous driving decisions through trajectory data. Paper Presented at 94th Annual Meeting of the Transportation Research Board.
- Kluger, R., Smith, B.L., Park, H., Dailey, D.J., 2016. Identification of safety-critical events using kinematic vehicle data and the discrete fourier transform. *Accid. Anal. Prev.* 96, 162–168.
- Kowalski, A., Martín, M., Plastino, A., Rosso, O., 2007. Bandt–Pompe approach to the classical-quantum transition. *Physica D* 233 (1), 21–31.
- Laureshyn, A., Svensson, Å., Hydén, C., 2010. Evaluation of traffic safety, based on micro-level behavioral data: theoretical framework and first implementation. *Accid. Anal. Prev.* 42 (6), 1637–1646.
- Langari, R., Won, J.S., 2005. Intelligent energy management agent for a parallel hybrid vehicle-part I: system architecture and design of the driving situation identification process. *IEEE Trans. Veh. Technol.* 54 (3), 925–934.
- Lee, J., Jang, K., 2017. A framework for evaluating aggressive driving behaviors based on in-vehicle driving records. *Transp. Res. Pt. F*. <https://doi.org/10.1016/j.trf.2017.11.021>.
- Li, J., Yan, J., Liu, X., Ouyang, G., 2014. Using permutation entropy to measure the changes in EEG signals during absence seizures. *Entropy* 16 (6), 3049–3061.
- Ma, Z., Sun, J., Wang, Y., 2017. A two-dimensional simulation model for modelling turning vehicles at mixed-flow intersections. *Transp. Res. C* 75 (75), 103–119.
- Ni, Y., Wang, M., Sun, J., Li, K., 2016. Evaluation of pedestrian safety at intersections: a theoretical framework based on pedestrian-vehicle interaction patterns. *Accid. Anal. Prev.* 96, 118–129.
- Parker, M., Zegeer, C.V., 1989. Traffic Conflict Techniques for Safety and Operations Observer's Manual. US Department of Transportation. Federal Highway Administration, McLean, Virginia.
- Ryder, B., Dahlinger, A., Gahr, B., Zundritsch, P., Wortmann, F., Fleisch, E., 2018. Spatial prediction of traffic accidents with critical driving events—Insights from a nationwide field study. *Transp. Res. Pt. A*. <https://doi.org/10.1016/j.tra.2018.05.007>.
- Suzuki, K., Nakamura, H., 2006. Traffic analyzer—the integrated video image processing system for traffic flow analysis. Proceedings of the 13th World Congress on Intelligent Transportation Systems.
- Saunier, N., Sayed, T., 2007. Automated analysis of road safety with video data. *Transp. Res. Rec.* 43 (2019), 51–56.
- Tageldin, A., Sayed, T., Ismail, K., 2018. Evaluating the safety and operational impacts of left-turn bay extension at signalized intersections using automated video analysis. *Accid. Anal. Prev.* 120, 13–27.
- Tageldin, A., Sayed, T., 2016. Developing evasive action-based indicators for identifying pedestrian conflicts in less organized traffic environments. *J. Adv. Transp.* 50, 1193–1208.
- Tageldin, A., Sayed, T., Shaaban, K., 2017. Comparison of time-proximity and evasive action conflict measures: case studies from five cities. *Transp. Res. Rec. J. Transp. Res. Board* 2661, 19–29.
- Vlahogianni, E.I., Yannis, G., Golias, J.C., 2014. Detecting powered-two-wheeler incidents from high resolution naturalistic data. *Transp. Res. F* 22 (1), 86–95.
- Wali, B., Khattak, A.J., Bozdogan, H., Kamrani, M., 2018. How is driving volatility related to intersection safety? A Bayesian heterogeneity-based analysis of instrumented vehicles data. *Transp. Res. C* 92, 504–524.
- Wang, X., Khattak, A.J., Liu, J., Masghati-Amoli, G., Son, S., 2015. What is the level of volatility in instantaneous driving decisions? *Transp. Res. C* 58, 413–427.
- World Health Organization, 2017. Road Traffic Injuries. From. <http://www.who.int/mediacentre/factsheets/fs358/en/>.